Spatiotemporal evaluation of future groundwater recharge in arid and semi-arid regions under climate change scenarios

Soghra Andaryani[a*], Biswajeet Pradhan[b,c,d], Vahid Nourani[a], Tahereh Jalali[e], Farnaz Ershadfath[f], Ali Torabi Haghighi[g]

[a] Center of Excellence in Hydroinformatics and Faculty of Civil Engineering, University of Tabriz, Tabriz, Iran

[b] Center for Advanced Modeling and Geospatial Information Systems (CAMGIS), Faculty of Engineering and Information Technology, University of Technology Sydney, NSW 2007, Australia

[c] Department of Energy and Mineral Resources Engineering, Sejong University, Choongmu-gwan, 209 Neungdong-ro, Gwangjin-gu, Seoul 05006, Korea

[d] Earth Observation Center, Institute of Climate Change, Universiti Kebangsaan Malaysia, 43600 UKM, Bangi, Selangor, Malaysia

[e] Department of Climatology, Faculty of Planning and Environmental Sciences, University of Tabriz, Tabriz, Iran

[f] Department of Agroecology, Aarhus University, Blichers Allé 20, 8830 Tjele, Denmark

[g] Water, Energy and Environmental Engineering Research Unit, University of Oulu, 90570, Oulu, Finland

[*] Corresponding author: e-mail: s.andaryani@gmail.com

Abstract

In this study, the Hydrologic Evaluation of Landfill Performance (HELP3.8D) model was developed to evaluate the spatiotemporal distribution of potential Groundwater recharge (GWR) in Tasuj aquifer, northwestern Iran. High-resolution future climatic data from CanESM2 General Circulation Models (GCMs) was produced under different scenarios of Representative Concentration Pathways (RCP2.6, RCP4.5, and RCP8.5). The analysis of climate parameters demonstrated that under RCP2.6, climatic variation will be substantially similar to that of the observed period (1961-2005), while moderate and severe droughts are anticipated under scenarios RCP4.5 and RCP8.5, respectively over 2017-2030. The projection results showed that GWR will be changed by climate change, on average, from 31 mm/yr at baseline to 32 (+3%), 28.5 (-8%) and 11.5 (-63%) mm/yr under the RCP2.6, RCP4.5 and RCP8.5

scenarios, respectively. This approach can be easily replicated by other researchers and could be beneficial for monitoring water security and managing groundwater resources in other catchment areas.

Keywords: Groundwater recharge; Climate change; HELP model; GIS; Tasuj plain aquifer, Iran.

Introduction

Based on the Fifth Assessment Report (AR5) of the Intergovernmental Panel on Climate Change (IPCC), the mean global surface temperature showed an increasing trend of 1°C by the end of 2018 (IPCC, 2018). On the other hand, precipitation in Asia showed a decreasing trend over the period 1880 to 2012 (Christensen et al., 2013). These changes in recent decades have affected water resources both directly (i.e., direct interaction with surface water resources) and indirectly (i.e., impacts on aquifer recharge and storage aquifers) (Jyrkama and Sykes, 2007; Xia and Chen, 2008; Toreti et al., 2009; Beigi et al., 2014; Bloomfield and Marchant, 2013). On the other hand, groundwater (GW) demand (e.g., GW used for agricultural, industrial, recreational, tourism, and residential activities) has more than doubled in recent decades. It will continue to rise in the future because of population growth, national development policies, reduced access to surface water, and climate change (Scibek and Allen, 2006; Scibek et al., 2007; Mayer and Congdon, 2008; Ghazavi and Ebrahimi, 2019). The lack of precipitation, and its uneven spatiotemporal distribution and increasing temperature rise, leads to considerable socio-economic and environmental challenges (Vaghefi et al., 2019; Panahi et al., 2020, Ashraf et al., 2021). Subsequently, GW plays a major role in supplying water demands (Nassiri et al., 2006; Abbaspour et al., 2009). Additionally, severe climate fluctuations and the occurrence of intermittent and long-term droughts in Iran have exacerbated water scarcity and highlighted the importance of GW management and planning (Zarghami et al., 2011; Ashraf et al., 2021). Accordingly, for water managers and policymakers to get a clear picture of future water availability, a precise projection of the impacts of climate change on groundwater recharge (GWR) is needed (Prinos et al., 2002; Andaryani et al., 2019b; Ashraf et al., 2021).

The number of research papers on GWR sensitivity to climate change using various physical, numerical, data-driven, machine learning and time series methods has skyrocketed in recent decades, summaries in the following review articles e.g., Earman and Dettinger., 2011; Treidel et al., 2012; Kløve et al., 2014; Pulido-Velazquez et al., 2015. The GWR sensitivity issue associated with the climate change has been studied in various research projects, which have shown reduction (e.g., Bouraoui et al., 1999; Candela et al., 2009; Andaryani et al., 2019a) as well as increase (e.g., Green et al., 2007; Jyrkama and Sykesa, 2007; Kovalevskii, 2007; Gurdak and Roe, 2010) in GWR due to climate change. Because of the complexity of the process, evaluating recharge as a direct measure is unreliable. The methods such as Hydrologic Evaluation of Landfill Performance (HELP) as a physical model are utilized to estimate GWR according to the data accessibility, expenses, area expansion, climate, etc. The efficiency of the HELP model (Schroeder and Peyton, 1987; Schroeder et al., 1994) in comparison to the others has been evaluated in numerous studies, which have proved the ability of this model to estimate GWR (Berger, 2000; Jyrkama et al., 2007; Toews and Allen, 2009; Beigi et al., 2014). For instance, Jyrkama and Sykes (2007) reported that the GWR rate would increase from 10 to 50% under CC in an area of 7000km^2 using the HELP model. Toews and Allen (2009) applied the HELP model in an arid and semi-arid climate (i.e., the Oliver region, British Columbia, Canada, with annual precipitation of 300mm) using geospatial data (i.e., soil, land use, surface slope, Leaf Area Index (LAI) and GW depth) for areas with a resolution of 100×100m to assess the climate change impact on irrigation-induced GWR. Based on their findings, irrigation return flow and GWR are predicted to increase by 0.4 and 4mm/day for the most and least efficient irrigation systems under scenarios of climate change. In a separate work, Zhang et al. (2016) used this model to simulate the capillary barrier covers (type of evapotranspiration (ET)) under high precipitation conditions. The results indicated an increase in capillaries under the studied condition in clay texture. Therefore, according the studies looked at here, the predicted changes in temperature and precipitation can have significant impacts on hydraulic heads, recharge rates, and capillary mechanisms (Green et al., 2007; Aguilera and Murillo, 2009; Kumar, 2012; Green, 2011; Meixner et al., 2016).

Here, HELP3.8D model was employed to evaluate the possible impacts of three Representative Concentration Pathways (RCP) for climate change scenarios (RCP2.6, RCP4.5, RCP8.5) on GWR in the Tasuj sub-basin of the Urmia Lake Basin (a hypersaline lake which is completely drying), Iran. Although some studies have been conducted to assess GWR under climate change, but less attention has been paid to GWR in arid and semi-arid regions with consideration of the uncertainty decrease through monthly LAI. In the previous studies, e.g., Toews and Allen (2009); Beigi et al. (2014), LAI values were considered separately for individual wells, without looking at the monthly LAI for the growing season. While monthly LAI can be applied in models suffering from the limitation of ET estimation, as their estimation is based on using the available water content in the evaporation depth zone (this zone specified by the user is non-physical-based depth parameter in the model) (Jyrkama et al., 2007; Toews and Allen, 2009). This zone is considered equal to the plant rooting depth which is determined by users. Consequently, LAI and its monthly variation can be the controlling factor for ET and GWR. On the other hand, GWR monitoring for managing water resources and identifying the suitability of groundwater quantity for irrigation purposes in arid and semi-arid areas of developing countries plains such as Iran has not been carried out properly. However, some large-scale projects have been focused on GW level decline under climatic and anthropogenic changes, as well as the interaction between lake water level (such as Lake Urmia) and GW level reduction (e.g., Jvadzadeh et al., 2020; Ashraf et al., 2021). To the best of our knowledge, GWR has not been analyzed under climate scenarios in this case study and the areas surrounding it that are suffering from the lack of proper data for modeling have not been assessed so far.

Therefore, the main objectives of our study are the projection of monthly, seasonally, and yearly spatiotemporal GWR and uncertainty reduction under different climate change scenarios using monthly LAI in Tasuj plain, an area which is experiencing a remarkable drop in the groundwater level (Fig. 1).

Fig.1

First, a Statistical Downscaling Model (SDSM) was used for reducing the scale of climatic variables provided by General Circulation Models (GCMs) (Wilby et al., 2002) under the three specified climate change scenarios. Second, the hydrological cycle variation was simulated in 24 piezometric wells located in the area. Then, monthly LAI obtained from Moderate Resolution Imaging Spectroradiometer (MODIS) product in the location of each well was utilized to decrease model uncertainty. Due to the unavailability of data for evaluation of the simulated GWR, the simulated ET was examined using the ET of MODIS product from 2001-2005. Subsequently, GWR was plotted against the observed GW level in this period. Finally, maps of spatiotemporal distribution of GWR were produced under the CC scenarios at a monthly, seasonal, and yearly scale. Results of our study can help to provide insight into possible future challenges related to water management in the study area. Particularly, generating the spatiotemporal maps under climate change can help us to understand the interaction between groundwater recharge and climate change in arid and semi-arid regions.

2. Data and method

In order to analyze the future groundwater recharge in a semi-arid region under climate change scenarios, a set of tasks, as presented in Fig. 2, were followed, comprising estimation of groundwater recharge and

ET using the HELP model, projection of climate change and projection of groundwater recharge under different climate change scenarios.

Fig. 2.

2.1. Study Area

This study was conducted in an intensively farmed sub-catchment of 602km^2 (36%, mainly farmland) of the 51800km^2 Urmia Lake's catchment, located in the East Azerbaijan Province of Iran between 45˚2′ E to 45˚32′ E longitude and 38˚11′ N to 38˚25′ N latitude (Fig. 3). The topographical elevation varies from 1510 to 3114m above sea level, and the region has flow from only eight seasonal rivers, without any permanent river. The annual mean precipitation and temperature are 276 mm/yr (2000-2012) and 12°C (1961-2014) available from Tasuj and Tabriz stations, respectively.

There is a significant diversity of geological formations in the study area. Among these, three igneous, metamorphic and sedimentary rocks can be found from the Precambrian period to the present (1:100,000 geology maps from Khodabandeh and AminiFazl, 1993). A significant area in the south of the plain has become saline due to the shrinkage of Lake Urmia (Fig. 3a). In this plain, the Quaternary alluvium is divided into alluvial terraces and alluvial fans, which are the sources of aquifer recharge in the plain. (Fig. 3b). The younger part is in the form of alluvial terraces and is usually located along rivers (flood plain) with a thickness of 30m (Nadiri et al., 2013). An unconfined and heterogeneous aquifer with an area of about 212.5km^2 (plain area of 258km^2), a storage coefficient of 3%, and precipitation infiltration (PI) of 3.3% is located in the younger section (Table 2 of Javadzadeh et al., 2020). The land use (LU) data used in this study was available from typical Iranian LU types, based on Sentinel-2 with a spatial resolution of

10m, where 13 typical LU types have been classified for the whole of Iran by Gorbanian et al., 2020 (Fig. 3c).

Fig. 3.

2.2. Input Data

Elevation, land use, soil data, plant, and climatic data were obtained from multiple sources and different time periods (Table 1).

Table 1.

Meteorological data, including the daily precipitation and temperature from 1961-2005, were introduced into the SDSM model to project climate variation (Fig. 4). Furthermore, the climate variables (i.e., precipitation, temperature, solar radiation, wind speed, and relative humidity) obtained from Tabriz synoptic station (46˚, 17´ E longitude and 38˚, 05´ N latitude) were used to calculate recharge and evapotranspiration in the HELP model.

Fig. 4.

To provide the soil data for modelling, we used information from 24 piezometric wells (e.g., Fig. 5a, Amestarjan well, namely W3). Fig. 5b presents the texture map for the soil's first layer and the location of the piezometric wells. Based on this map, soil textures were sandy, sandy-clay, sandy-silty, and sandy-silty-clay. The depth of soil texture decreases gradually from the north to south of the region. For instance, the information from one of the piezometric logs of soil texture showed different textures at various depths, 0-15m (sandy), 15-30m (gravel and clay), 30-45m (gravel with clay), 55-48m (silt with sand), 48-66m (sand-gravel-clay), 66-69m (gravel-sand with clay) and 69-79m (gravel with sand). It should be noted that the initial layer depth of the unsaturated zone in the piezometric logs was considered as the layer thickness (see Fig. 5a).

Fig. 5.

The runoff curve number (CN) as a necessary parameter in the estimation of runoff depends on the vegetation cover, cultivated area, type of agricultural operations, soil moisture conditions, soil permeability and plant rooting depth (Hawkins, 1978). The CN for the area was calculated as the weighted average based on the surface cover characteristics of the study area and the soil hydrological group under moderate moisture conditions (Zhan and Huang, 2004).

Based on the information available in the Agricultural Organization of Tasuj city (Iranian Ministry of Jahade-Agriculture (MOJA, 2007)), the most significant agricultural lands in the plain are allocated to wheat, tomato, and apricot production. The growing seasons for spring and winter wheat are from April to May and from September to November, respectively, while the growing season for summer crops and orchards is from June to September. Given that the depth of the evaporation zone (i.e., the maximum depth of consuming ET) should be at least equal to the average depth of plant root penetration, to determine the depth of root penetration of wheat, summer crops and orchard plants, we considered both the estimations of the root penetration depth on a global scale (Canadell et al., 1996) and the comments of agricultural experts in the Tasuj plain. Depending on the soil thickness and types of topsoil and cultivated plant, the root penetration depth was estimated to be about one to three meters.

Considering that a plant-covered surface has more ET under similar conditions than a plant-free surface (Andaryani et al., 2021), the vegetation cover is another important factor affecting the amount of groundwater and its storage. Therefore, in this study, we used the Leaf Area Index (LAI) obtained from MODIS products (i.e., MOD15A3H.006), defined as the one-sided green leaf area per unit of ground surface area on a four-day temporal scale. LAI has been extracted for the locations of all 24 wells (Fig. 6, which shows the LAI in the growing season of 2003).

Fig. 6.

2.3. Investigation of future climate change through statistical downscaling of global climate projection

In order to project climate variables on smaller scales, such as a watershed or in urban areas, the outputs of Atmospheric General Circulation Models (AGCM) must be downscaled using dynamic models and/or statistical methods (Wilby and Dawson, 2007). Given that the dynamic models are costly, researchers' attention has been drawn to SDSM, which involves expanding quantitative relationships between large-scale atmospheric and local variables. In the present study, the SDSM, which works based on multiple linear regression and the stochastic weather generator, was applied to downscale the general atmospheric circulation model (Wilby et al., 2002). The main advantages of this method are its simplicity, high speed, and economic justification in the downscaling process (Baghanam et al., 2019; Nourani et al., 2019). Statistical downscaling involves the expansion of quantitative relationships between large-scale atmospheric variables (predictors) and local variables (predictand) (Wilby and Dawson, 2007). The predictors can characterize different atmosphere features such as circulation, stability, thickness, and moisture content at various levels (500 hpa, 850 hpa and near the surface) (Getachew, 2021). It should be mentioned that the results of 4 GCMs models including ACCESS-1 (the Australian Community Climate and Earth System Simulator), MIROC-ESM (Model for Interdisciplinary Research on Climate), MIROC-

ESM-CHEM (An atmospheric chemistry coupled version of MIROC-ESM) and CanESM2 (second-generation Canadian Earth System Model) were compared together using Tailor diagram (Taylor, 2001) considering Correlation Coefficient (CC), Standard Deviation (SD) and Root Mean Square Error (RMSE) between historical data of the models and observed data (Fig.7). According to the Fig. 7, historical of CanESM2 is closer to observed data. On the other hand, previous studies have , also, shown that the CanESM2 developed by the Canadian Centre for Climate Modelling and Analysis (CCCma) of Environment Canada is capable of simulating the climate for the arid and semi-arid climate of Iran (Emami and Koch, 2018; Zamani and Berndtsson, 2019; Saatloo et al., 2020); therefore, this model, with a spatial resolution of 2.8125° (longitude) × 2.8125° (latitude), was chosen to simulate future climate data under the three scenarios, RCP2.6, RCP4.5 and RCP8.5. Consequently, downscaling was done by applying 26 predictors of NCEP (National Centers for Environmental Prediction) reanalysis data for historical information (1961–2005) and CanESM2 for the future (2017–2030).

Fig. 7

Table 2 indicates the selected NCEP based on the high value of absolute correlation and partial correlation for CanESM2 model. In other words, the best predictor variables that have the highest correlation with the observed data (temperature, precipitation) logically and statistically were selected for projection.

Table 2.

The required data for projection was downloaded from the website https://esgf-node.llnl.gov/projects/cmip5 (see Table 2). The comparison of observed and historical data pertaining to CanESM2 based on NCEP's Table 2 is presented in Fig. 8.

Fig. 8

2.4. Recharge calculation model

2.4.1. HELP model

HELP as a quasi-two-dimensional model (i.e., HELP 3.8, a DOS-based software, refer to Schroeder et al., 1994 for more detail) was employed to assess GWR. The model simulates all the surface and subsurface hydrological processes to estimate the daily movement of water using water balance equation (Eq. 1).

$$R = P - D - ET_a - \Delta W \quad (1)$$

Where, R is potential recharge, P represents precipitation, D is net runoff, Et is actual evapotranspiration and ΔW represents change in a soil water storage (for more detail refer to Lee et al, 2006).

The model used the SCS curve number approach to determine daily surface runoff (Eq. 2).

$$Q = \frac{(P - I_a)}{P - I_a + S} \text{ for P} \geq I_a \quad (2)$$

Where Q is runoff (mm), P is rainfall (mm), S is the potential maximum soil moisture retention after the beginning of runoff (mm), Ia represents the initial abstraction (mm), or the amount of water before runoff, such as infiltration, or rainfall interception by vegetation; and Ia= 0.2S is commonly assumed. The following equation is used to compute the CN:

$$\text{CN} = \frac{1000}{S} - 10 \quad (3)$$

The CN scale runs from 0 to 100, with lower values indicating reduced runoff potential and higher numbers indicating more runoff potential. Soil type, soil infiltration capabilities, land usage, antecedent soil moisture content, and seasonal water table depth are all factors that influence the CN. In addition, the FAO Penman-Monteith method (Allen et al., 1998) is used to determine the reference evapotranspiration. The processes start with the calculation of the surface water budget, ET, investigation of water infiltration, and water routing to the last and deepest soil layer. In this regard, the model considered a soil column as comprising several layers from the surface to the water table and determined the daily infiltration in each layer directly using the surface water budget. Here, we reported only ET and recharge of the case study.

2.4.2. Accuracy of the HELP results

In this study, due to the absence of observed runoff and ET data to validate the model results, the estimated ET data from the MOD16 with a spatial resolution of 500m were compared with computed ET from the HELP model. Five wells were selected to ensure the model results based on the completeness of their monthly scale data from April to September (the growing season) from 2001 to 2005 (Fig. 9, which shows only 2001 and 2005). Furthermore, the observed groundwater level was compared with the calculated recharge from HELP in this period. We could access to the complete data of GW level in five wells during the period of 2001-2005 for validating the model simulation.

As recharge data was not readily available in the study area, direct model calibration was only possible visually. Therefore, the accuracy of the estimated data was assessed using ET and recharge data.

Fig. 9.

3. Results and discussion

3.1. Projection of climate change over 2017-2030

Observed temperature and precipitation data (1961-2005) were compared to the outcomes of constructed data under various climate change scenarios to determine the possibility of future climate change (2017-2030). As seen in Fig. 10a, the temperature increases in scenario RCP8.5, which occurs over the cold months (Jan. to Mar. and Oct. to Dec.) and is higher than the other scenarios. The highest and lowest temperature rise will occur in Feb. and May, respectively. Under RCP4.5, the temperature will only decrease in April, however, it will increase in the other months. In addition, under RCP2.6, the temperature will decrease over the cold periods of each year compared to the baseline, with the highest values in March and April (0.2 and 0.25, respectively). In climate change scenarios, RCP2.6 is an optimistic pathway in which CH_4 emission in 2100 will be half of that in 2020, and CO2 emission will be nil (IPCC, 2018). However, based on, RCP4.5 and RCP8.5 all the months would experience a temperature increase apart from April under RCP4.5.

Fig. 10.

Fig. 10b shows precipitation changes under scenarios RCP2.6, RCP4.5, and RCP8.5 from 2019-2030 compared to the baseline. Even though precipitation does decrease over the warm seasons of the year, the decline is negligible compared to the precipitation reduction during the cold seasons. Under the RCP2.6 scenario, precipitation increases in the year's cold months and decreases in the warm months. In the other words, Precipitation, like temperature, demonstrates an improvement in the climate status of the research area under RCP2.6, i.e., precipitation will increase in six months of the year. The amount of precipitation under the RCP8.5 scenario is significantly reduced in all months. The maximum precipitation reduction under RCP8.5, RCP4.5 and RCP2.6 scenarios are -8.3, -4.49 and -2.9, respectively.

3.2. Comparison of MODIS ET and simulated ET using HELP under mean monthly and mean yearly LAI values

The model's sensitivity to parameters and input data is checked to provide better and more accurate results. Here, the effect of LAI changes as an input parameter of the HELP model on the recharge changes was investigated. As the density of the vegetation canopy influences plant transpiration, LAI can be used to show ET fluctuations.

Table 3 shows the values of recharge and ET with changes in LAI. As the table shows, there is an inverse relationship between LAI and recharge. LAI values of 0.1 and 5 correspond to the maximum and minimum levels of ET and recharge, respectively. These relationships for ET, LAI, and groundwater recharge have also been reported by Batelaan and De Smedt (2007) and Simic et al. (2014). Furthermore, for LAI values greater than 3, ET accounts for more than 90% of precipitation.

Table 3.

Due to the model's sensitivity to LAI (see Table 3), the values of this index were obtained from MODIS products. To increase the accuracy of the model, Mean Yearly Value (MYV) and Mean Monthly Value (MMV) of LAI for the location of each well (one corresponding pixel of MODIS is 25ha) were examined in the modeling process. Then, the simulated ET using the HELP model was evaluated against the ET of the MODIS product. Fig. 10 depicted the comparison between ET product and simulated ET in 5 selected wells over six months (the growing season) of each year in 2001-2005.

Fig. 11.

Since the maximum value of the LAI in the studied region occurs from April to September (i.e., the growing season), the mean monthly and yearly values of this period were used in modeling over the period 2001-2005 (see Fig. 11a). According to Fig. 11b, ET can be estimated more accurately by considering the spatiotemporal changes in LAI. In other words, when the mean monthly LAI is used for the location of each well, the correlation coefficient between MODIS-ET and simulated ET increases accordingly. It should be mentioned that the amount of ET accounts for more than 76% and 73% of precipitation for the mean monthly and yearly LAI, respectively.

Among the selected wells (Fig. 11), the highest correlations between predicted ET and those derived from MODIS images were ascribed to wells No. 12 and 14, respectively. These wells also have the highest LAI value during the growing season (see Fig. 6). The lowest correlation between estimated ET, and those generated from the MODIS product was seen in W5, which could be attributed to the well's soil texture. As shown in Fig. 5b, the soil texture around this well is sandy, allowing water to penetrate quickly into the lowest parts of the soil and reducing the chances of plant transpiration. Because geological and soil properties are considered in physical-based hydrological modeling, comparing simulated ET to satellite-based ET products, which are primarily dependent on ambient temperature and vegetation characteristics, etc., displays a lower correlation coefficient.

Here, our proposed model only takes into account the amount of evaporation caused by precipitation (i.e., we ignored the obtained recharge from irrigation due to lack of data); for this reason, the amount of evaporation in dry months of the year was estimated to be zero (see Fig. 11, the months of June, July and August). On the other hand, 1-dimensional models (pseudo-2-D) such as HELP do not calculate the path of surface water (and sub-surface water) between adjacent network cells (Jyrkama and Sykes, 2007; Toews and Allen, 2009). Crop irrigation evaporation and the path of surface water between the close network cells are, however, considered in ET estimation of MODIS. Therefore, the amount of computational ET with MODIS images is higher than that of the HELP model. Regardless of the differences between the MODIS and HELP model results, the general ET trend in both methods is consistent. This comparison can demonstrate the model's performance in recharging simulation. As previously stated, ET and recharge are inversely connected. Hence, correct ET simulation is proof of accurate recharge simulation.

3.3. Comparison of observed groundwater level and simulated recharge

Based on Fig. 12a, between 2001 and 2005, a hydrographic survey of selected wells in the Tasuj catchment area revealed a continuous reduction in groundwater level. It's worth noting that, in addition to rising temperature, increasing evaporation capacity, reducing rainfall, agricultural development, land-use change, and the use of groundwater resources as the primary source of domestic, industrial, and agricultural requirements have all had significant impacts on water level reduction in recent decades.

Although the increasing and decreasing trends of temperature and precipitation during 2001-2005 are not particularly noticeable (Fig. 12b), long-term study of temperature and precipitation changes from 1961-2005 (Fig. 3) demonstrates the decreasing trend of precipitation and increasing trend of temperature, which can have considerable impacts on water resource instability. In their investigations, Zarghami et al. (2011) and Nourani et al (2021) found increasing and decreasing trends in temperature and precipitation in the Urmia Lake basin. The purpose of comparing the level of selected wells and recharge is to evaluate the model's performance because the lower the groundwater recharge, the lower the groundwater level per unit time. It should be noted that factors such as uncontrolled groundwater abstraction are effective in lowering the groundwater level. Fig. 12 shows that the simulated groundwater recharge trend is nearly identical to the groundwater level trend, indicating that the model can perform well in simulating groundwater recharge in the future. It should be noted that We do not attempt to determine a direct mathematical relationship between groundwater level and GWR, but we know that there is a close relationship conceptually. Hence, supporting that the simulated signals of GWR in our scenarios are also representative of the likely changes in groundwater level in future scenarios.

Fig. 12.

3.5. Projected recharge under different climate change scenarios

As previously mentioned, the HELP model was used to estimate the amount of nutrition in the baseline period (1961-2005) and under climate change scenarios in the future period (2017-2030). This model can simulate the load of nutrition in the unsaturated zone of the soil, which works based on the water balance equation. Fig. 13 shows the mean monthly recharge over baseline and scenario periods. Under the RCP2.6 scenario, groundwater recharge in the rainy months (March to May) shows a small increase compared to the baseline due to increasing precipitation (see Fig. 10); the recharge peak in all wells, particularly in W14 and W15, through which many branches of the seasonal river flows, occurs in April, the baseline period. The maximum quantity of recharge in these wells is due to the practically permeable nature of the soil (sandy-clay), proximity to the mountains, and lower use of these wells for irrigation (see Fig. 5, which illustrates the low LAI in the vicinity of these wells). Due to the skinny soil layer (7m), soil texture (sandy-silty), and distance from seasonal sub-branches, well 8 has the lowest yearly recharge under this scenario from 2017 to 2030 (see Fig. 5b).

In comparison to the baseline, wells 8 and 14 will experience an annual recharge decrease and increase of 1.08 mm/yr and +4 mm/yr, respectively. Since the HELP model did not account for irrigation return flow, no recharge has been presented for the 2.6 and baseline scenarios for the June to September dry months, even though irrigation return flow may slightly replenish the well. Under the RCP4.5 and RCP8.5 scenarios, temperature increases in the cold months, resulting in precipitation transformation from snow to rain. Snowmelt reduction causes the recharge peak to shift from April to March in winter. This issue is particularly noticeable in well 14 (Fig. 13). Compared to the baseline period, the amount of recharge in the RCP4.5 and RCP8.5 scenarios will be much lower. The recharge amount in most wells will be severely reduced under the RCP8.5 scenario due to lower rainfall and a large increase in temperature (see Fig. 10). Most wells will be refilled at a rate of less than 3 mm/yr in this scenario. As previously noted, the reason for the largest recharge in Wells 14 and 15 is more dependent on the geological structure and soil texture of the examined wells, as well as their location, which has caused the rate of penetration of these wells to be higher than the other wells in the baseline period and under the three studied scenarios.

Fig. 13.

According to Fig. 14, which shows the seasonal recharge of piezometric wells in the baseline and under climatic scenarios, the seasonal distribution of well recharge follows the rainfall pattern in the region. The maximum recharge occurs in spring in the baseline and RCP2.6 scenarios; however, under the RCP4.5 scenario, and especially the RCP8.5 scenario, it happens in winter, indicating a shift in maximum recharge from spring to winter. As previously stated, in the simulation using the HELP model, the dry season does not affect the recharge of the examined wells, and the recharge rate in this season is zero. Due to the decrease in initial soil moisture over the summer and autumn, the recharge process will probably begin in the winter, with a time delay in both scenarios RCP4.5 and RCP8.5. The seasonal recharge decline trend in the baseline period explores the following pattern: Spring> winter> autumn> summer; however, in the RCP8.5 scenario, there is no recharging in summer and autumn, and the quantity of recharge in the other seasons will reduce significantly. In general, the quantity of net recharge in this coastal aquifer is minimal due to the high ET rate. In addition to the effects of climate change, this ET rate may be attributed to the overdevelopment of cultivated land (agricultural expansion) over a long period without considering the balanced development of pressured irrigation systems in this basin. Under RCP4.5 and RCP8.5 scenarios, aquifer recharge is active for a short period during the winter when the plants are dormant and ET activity is at its lowest level. In the spring and autumn, a significant portion of the precipitation evaporates, while the remainder is converted to runoff or soil moisture, with just a tiny portion being converted into groundwater recharge.

Fig. 14.

Regarding annual spatial changes (Fig.15) under climate scenarios, groundwater recharge in the western half of the region will experience a sharp decline. Recharge varied from 15mm in the east of the basin to 47mm in the west over the baseline period, while, with increasing precipitation in RCP2.6 scenario, the amount of recharge will increase slightly compared to the baseline period and will experience a minimum and maximum difference of 1 and 2mm, respectively. Topographic characteristics and recharging wells from seasonal rivers are the reasons for higher recharge in the western part of the aquifer. Water penetration is also affected by the type of soil texture. The changes in spatial recharge for the period 2017-2030 under the RCP4.5 and RCP8.5 scenarios are the same as the baseline period, however, the quantity of recharge will decrease in both scenarios. Due to a decline in precipitation and a severe rise in temperature (up to 0.4℃ obtained from Fig. 10), the recharge caused by precipitation in the RCP8.5 scenario will be significantly lower than in the RCP2.6 and RCP4.5 scenarios (Up to 25mm/yr difference from the baseline). Under this pessimistic scenario, the drying up of wells and the destruction of the aquifer is anticipated. The method provided here can be applied to a variety of aquifers in various climate zones, particularly in arid areas. Using this approach, wells that are prone to drying can be identified. Therefore, various methods, such as artificial recharge, controlled groundwater abstraction, applying improved irrigation systems and cultivating crops that do not require irrigation in the summer, can all be employed to maintain aquifers and avoid future consequences like subsidence in the plains.

Fig. 15.

4. Conclusion

To study the impact of climatic factors such as variation in water resources, especially groundwater directly through interactions between rivers and lakes and indirectly through groundwater recharge, GWR for the near future (2017-2030) was simulated under three climatic scenarios. Based on the results of this study, the following conclusions could be drawn:

- Since the effect of climate change on various hydrological components is nonlinear, it is critical to consider the different characteristics of an area, such as soil texture and thickness, vegetation, and the other unique aquifer features in various sections (here, the different characteristics of 24 piezometric wells were considered).
- Using satellite data to validate the model in locations where data is scarce can be beneficial.
- Except for the RCP2.6 scenario, climate change scenarios in the study area predict temperatures rising and precipitation decreasing during the cold seasons and the rainy months (spring), respectively. These changes will reduce snowfall and indirectly affect the most important groundwater supply source (i.e., snowmelt affects runoff, which affects groundwater supply). Also, global warming and reduced precipitation will diminish groundwater recharge directly.
- Hydrological modeling using HELP, with consideration of the LAI value on a monthly basis for each well, for the RCP8.5 scenario shows a very sharp decrease in GWR of at least 14mm/yr and a maximum of 25mm/yr (50% and 93%, respectively) compared to the baseline period.
- In the RCP4.5 scenario, reduction in GWR reaches a total of 13%. However, the RCP2.6 scenario is optimistic, predicting a 5% increase in recharge.

- The anticipated decline trend of GWR in the study region under climate scenarios is similar to the baseline, and it moves from west to east, which could be attributable to soil type or present land use (agricultural is more developed in the study area's east).

In this study, land-use change corresponding to climate change was not taken into account for the future period based on LAI and irrigation. It is suggested that the amount of aquifer recharge under the influence of land-use changes, population growth, the increasing water demand of plants due to rising temperatures, and other factors be explored in future studies.

References

Abbaspour, K.C., Faramarzi, M., Seyed Ghasemi, S., Yang, H., 2009. Assessing the impact of climate change on water resources in Iran. Water Resources Research 45(10). https://doi.org/10.1029/2008WR007615

Aguilera, H., Murillo, J., 2009. The effect of possible climate change on natural groundwater recharge based on a simple model: a study of four karstic aquifers in SE Spain. Environmental Geology volume 57(5), 963–974

Allen, R.G., Pereira, L.S., Raes, D., Smith, M., 1998. Crop evapotranspiration: guidelines for computing crop requirements. FAO Irrigation and Drainage Paper No. 56. FAO, Rome, Italy.

Andaryani S, Nourani V, Trolle D, Dehghani M, Mokhtari AM., 2019. Assessment of land use and climate change effects on land subsidence using a hydrological model and radar technique. Journal of Hydrology 578:124070, DOI: https://doi.org/10.1016/j.jhydrol.2019.124070

Andaryani, S., Trolle, D., Nikjoo, M.R., Rezaei Moghadam, M.H., Mokhtari, D., 2019. Forecasting near future impacts of land use and climate change on the Zilbier River hydrological regime, northwestern. Iran. Environ. Earth Sci. 188 (6). https://doi.org/10.1007/s12665-019-8193-4

Ashraf, S., Nazemi, A., AghaKouchak, A., 2021. Anthropogenic drought dominates groundwater depletion in Iran. Scientific reports-Nature portfolio 11(1). https://doi.org/10.1038/s41598-021-88522-y.

Baghanam, A.H., Nourani, V., Keynejad, M.A., Taghipour, H., Alami, M.T., 2019. Conjunction of wavelet-entropy and SOM clustering for multi-GCM statistical downscaling. Hydrology Research 50 (1), 1–23.

Batelaan, O., De Smedt, F., 2007. GIS-based recharge estimation by coupling surface-subsurface water balances. Journal of Hydrology 337, 337-355.

Beigi, E., Frank T.-C. Tsai., 2014. GIS-Based Water Budget Framework for High-Resolution Groundwater Recharge Estimation of Large-Scale Humid Regions. Journal of Hydrologic Engineering 19(8). https://doi.org/10.1061/(ASCE)HE.1943-5584.0000993.

Berger, K., 2000. Validation of the hydrologic evaluation of landfill performance (HELP) model for simulating the water balance of cover systems. Environmental Geology 39 (11), 1261–1274.

Bloomfield, J.P., Marchant, B.P., 2013. Analysis of groundwater drought building on the standardized precipitation index approach. Hydrology Earth System Science. 17, 4769–4787. https://doi.org/10.5194/hess-17-4769-2013.

Bouraoui, F., Vachaud, G., Li, L.Z.X., Le Treut, H., Chen, T., 1999. Evaluation of the impact of climate changes on water storage and groundwater recharge at the watershed scale. Climate Dynamics 15(2), 153–161.

Canadell, J., Jakson, R.B., Ehleniger, J.R., Mooney, H.A., Sala, O.E., Schulze, E.D. 1996. Maximum rooting depth of vegetation type at the global scale, Oecologia, 108, 583-595.

Candela, L., Igel V.W., Elorza F.j., Aronica, G., 2009. Impact assessment of combined climate and management scenarios on groundwater resources and associated wetland (Majorca, Spain). Journal of Hydrology 376(3–4), 510–527.

Christensen, J.H., K. Krishna Kumar, E. Aldrian, S.-I. An, I.F.A. Cavalcanti, M. de Castro, W. Dong, P. Goswami, A. Hall, J.K. Kanyanga, A. Kitoh, J. Kossin, N.-C. Lau, J. Renwick, D.B. Stephenson, S.-P. Xie and T. Zhou, 2013: Climate Phenomena and their Relevance for Future Regional Climate Change Supplementary Material. In: Climate Change 2013: The Physical Science Basis. Contribution of Working Group I to the Fifth Assessment Report of the Intergovernmental Panel on Climate Change [Stocker, T.F., D. Qin, G.-K. Plattner, M. Tignor, S.K. Allen, J. Boschung, A. Nauels, Y. Xia, V. Bex and P.M. Midgley (eds.)]. Available from www.climatechange2013.org and www.ipcc.ch.

Earman, S., Dettinger, M., 2011. Potential impacts of climate change on groundwater resources – a global review. Journal of Water and Climate Change 2 (4), 213–229.

Emami, F., Koch, M., 2018. Evaluation of Statistical-Downscaling/Bias-Correction Methods to Predict Hydrologic Responses to Climate Change in the Zarrine River Basin, Iran. Climate, 6 (2), 30. https://doi.org/10.3390/cli6020030

Getachew, B., Manjunatha, B.R., Gangadhara, H.B., 2021. Modeling projected impacts of climate and land use/land cover changes on hydrological responses in the Lake Tana Basin, upper Blue Nile River Basin, Ethiopia. Journal of Hydrology 595, 125974, https://doi.org/10.1016/j.jhydrol.2021.125974.

Ghazavi, R., Ebrahimi, H., 2019. Predicting the impacts of climate change on groundwater recharge in an arid environment using modeling approach. International Journal of Climate Change Strategies and Management 11 (1), 88-99.

Ghorbanian, A., Kakooei, M., Amani, M., Mahdavi, S., Mohammadzadeh, A., Hasanlou, M., 2020. Improved land cover map of Iran using sentinel imagery within google earth engine and a novel automatic workflow for land cover classification using migrated training samples. ISPRS Journal of Photogrammetry and Remote Sensing, 167, 276–288.

Green, T.R., Bates, B.C., Charles, S.P., Fleming, P.M., 2007. Physically based simulation of potential effects of carbon dioxide-altered climates on groundwater recharge. Vadose Zone Journal 6(3), 597–609.

Green, T.R., Taniguchi, M., Kooi, H., Gurdak, J.J., Allen, D.M., Hiscock, K.M., Treidel, H., Aureli, A., 2011. Beneath the surface of global change: impacts of climate change on groundwater. Journal of Hydrology 405(3–4), 532–560.

Gurdak, J.J., Roe, C.D., 2010. Review: recharge rates and chemistry beneath playas of the High Plains aquifer USA. Hydrogeology Journal 18(8), 1747–1772.

Hawkins, R.H., 1978. Effects of rainfall intensity on runoff curve numbers, Proc., 1978, Meeting of the Arizona Section of the AM. Hydrology and Water Resources in Arizona and the Southwest 8, Arizona-Nevada Academy of Science, 53-64.

Intergovernmental Panel on climate Change (IPCC), 2018. Summary for policymakers: Global warming of 1.5 °C—An IPCC Special Report on the impacts of global warming of 1.5 °C above pre industrial levels and related global greenhouse gas emission pathways, in the context of strengthening the global response to the threat of climate change, sustainable development, and efforts to eradicate poverty, V. Masson-Delmotte et al., Eds, www.ipcc.ch/report/sr15 (IPCC, World Meteorological Organization, United Nations Environment Programme, Geneva, Switzerland).

Iranian Ministry of Jahade-Agriculture (MOJA)., 2007. Agricultural Statistics and the Information Center, Tehran, Iran.

Javadzadeh, H., Ataie-Ashtiani, B., Hosseini, S.M., Simmons, C.T., 2020. Interaction of lake-groundwater levels using cross-correlation analysis: A case study of Lake Urmia Basin, Iran, Science of the Total Environment, https://doi.org/10.1016/ j.scitotenv.2020.138822

Javadzadeh, H., Ataie-Ashtiani, B., Hosseini, S.M., T. Simmons, C., 2020. Interaction of lake-groundwater levels using cross-correlation analysis: A case study of Lake Urmia Basin, Iran. Science of the Total Environment, https://doi.org/10.1016/ j.scitotenv.2020.138822.

Jyrkama, M.I., Sykes, J.F., 2007. The impact of climate change on spatially varying groundwater recharge in the grand river watershed (Ontario). Journal of Hydrology 338(3–4),237–250.

Khodabandeh, A. A; Amini-Fazl, A., 1993. Geological map of Tasuj sheet (1:100,000). Geological Survey of Iran.

Kløve, B., Ala-Aho, P., Bertrand, G., Gurdak, J. J., Kupfersberger, H., Kværner, J., Muotka, T., Mykrä, H., Preda, E., Rossi, P., Uvo, C. B., Velasco, E., Pulido-Velazquez, M., 2014. Climate change impacts on groundwater and dependent ecosystems. Journal of Hydrology, 518 (Part B), 250- 266. https://doi.org/10.1016/j.jhydrol.2013.06.037

Kovalevskii, V.S., 2007. Effect of climate changes on groundwater. Water Recourses 34(2),140–152.

Kumar, C. P., 2012. Climate Change and Its Impact on Groundwater Resources. International Journal of Engineering and Science 1 (5), 43-60.

Lee, C., Chen, W., Lee, R. 2006. Estimation of groundwater recharge using water balance coupled with base-flow-record estimation and stable-base-flow analysis. Environmental Geology 51, 73–82.

Mayer, T.D., and R.D. Congdon. 2008. Evaluating climate variability and pumping effects in statistical analyses. Ground Water 46, 212-227.

Meixner, T., Manning, A. H., Stonestrom, D. A., Allen, D. M., Ajami, H., Blasch, K. W., Brookfield, A.E., Castro, C.L., Clark, J.F., Gochis, D.J., Flint, A.L., Neff, K.L., Niraula, R., Rodell, M., Scanlon, B.R., Singha, K., Walvoord, M.A., 2016. Implications of projected climate change for groundwater recharge in the western United States: review paper. Journal of Hydrology 534 124–138.

Nadiri, AA., Moghaddam, AA., Tsai, FT., Fijani, E., 2013. Hydrogeochemical analysis for Tasuj plain aquifer, Iran. Journal of earth system science 122(4),1091–1105.

Nassiri, M., Koocheki, A., Kamali, G. A., Shahandeh, H., 2006. Potential impact of climate change on rainfed wheat production in Iran. Archeves of Agronomy and Soil Sciences 52, 113–124.

Nourani, V., Paknezhad, N.J., Sharghi, E., Khosravi, A., 2019. Estimation of prediction interval in ANN-based multi-GCMs downscaling of hydro-climatologic parameters. Journal of Hydrology, https://doi.org/10.1016/j.jhydrol.2019.124226.

Nourani, V., Tootoonchi, R., Andaryani, S., 2021. Investigation of climate, land cover and lake level pattern changes and interactions using remotely sensed data and wavelet analysis. Ecological Informatics 64, 101330. https://doi.org/10.1016/j.ecoinf.2021.101330.

Panahi, D.M., Kalantari, Z., Ghajarnia, N., Seifollahi Aghmiuni, S., Destouni, G., 2020. Variability and change in the hydro-climate and water resources of Iran over a recent 30-year period, Scientific Reports volume 10, Article number: 7450

Prinos, S.T., Lietz, A.C., Irvin, R.B., 2002. Design of a real-time ground-water level monitoring network and portrayal of hydrologic data in southern lorida. Geological Survey (US) 18 (5), 2001-4275. https://doi.org/10.3133/wri20014275

Pulido-Velazquez, D., García-Aróstegui, J.L., Molina, J.L., Pulido-Velazquez, M., 2015. Assessment of future groundwater recharge in semi-arid regions under climate change scenarios (Serral-Salinas aquifer, SE Spain). Could increase rainfall variability increase the recharge rate? Hydrology Process. 29, 828–844.

Saatloo, S.M.E., Siosemarde, M., Hosseini, S.A., Rezaei, H., 2020. Variability assessment of simulated recharge resulted from precipitation using different GCMs, case study: west shore of Lake Urmia, Iran. Arabian Journal of Geosciences13, 610. https://doi.org/10.1007/s12517-020-05567-5

Schroeder, P. R., Peyton, R. L., 1987. Verification of the Hydrologic Evaluation of Landfill Performance (HELP) model using field data. Rep. EPA/600/S2-87/050, U.S. EPA, Cincinnati.

Schroeder, P.R., Dozier, T.S., Zappi, P.A., McEnroe, B.M., Sjostrom, J.W., Peyton, R.L., 1994. The Hydrologic Evaluation of Landfill Performance (HELP) Model: Engineering Documentation for Version 3. EPA/600/R-94/168b, US Environmental Protection Agency Office of Research and Development, Washington, DC.

Scibek, J., Allen, D.M., 2006. Comparing modelled responses of two high-permeability unconfined aquifers to predicted climate change. Global and Planetary Change 50, 50–62.

Scibek, J., Allen, D.M., Cannon, A.J., Whitfield, PH., 2007. Groundwater-surface water interaction under scenarios of climate change using a high-resolution transient groundwater model. Journal of Hydrology 333(2–4),165–181.

Simic, A., Fernandes, R., Wang, S., 2014. Assessing the Impact of Leaf Area Index on Evapotranspiration and Groundwater Recharge across a Shallow Water Region for Diverse Land Cover and Soil Properties. Journal of Water Resource and Hydraulic Engineering 3, 60–73.

Taylor, K.E., 2001. Summarizing multiple aspects of model performance in a single diagram. Journal of Geophysical Research: Atmospheres 106 (D7), 7183–7192.

Toews, MW., Allen, D.M., 2009. Evaluating different GCMs for predicting spatial recharge in an irrigated arid region. Journal of Hydrology 374(3), 265–281.

Toreti, A., Fioravanti, G., Percontia, W., Desiato, F., 2009. Annual, seasonal precipitation over Italy from 1961 to 2006. Int. J. Climatol. 29, 1976–1987. https://doi.org/ 10.1002/joc.1840.

Treidel, H., Bordes, J.J., Gurdak, J.J., 2012 (1st Edition). Climate change effects on groundwater resources: A global synthesis of findings and recommendations, IAH - International Contributions to Hydrogeology, Taylor and Francis publishing, 414 p.

Vaghefi, S.A., Keykhai, M., Jahanbakhshi, F., heikholeslami, J., Ahmadi, A., Hong, Y., Abbaspour, K. C., 2019. The future of extreme climate in Iran, Scientific Reports volume 9, Article number: 1464.

Wilby, R. L., Dawson, C. W., and Barrow, E. M., 2002. SDSM- a decision support tool for the assessment of regional climate change impacts, Environmental Modelling & Software., 17, 145-157.

Wilby, R.L., Dawson, C.W., 2007. SDSM 4.2-A Decision Support Tool for the Assessment of Regional Climate Change Impacts, User Manual.

Xia, J. Zhang, Y. 2008, water security in north China and countermeasure to climate change and human activity. Phys. Chem. Earth 33, 359-363.

Zamani, R., Berndtsson, R., 2019. Evaluation of CMIP5 models for west and southwest Iran using TOPSIS-based method. Theoretical and Applied Climatology 137, 533–543. https://doi.org/10.1007/s00704-018-2616-0

Zarghami, M., Abdi, A., Babaeian, I., Hassanzadeh, Y., 2011. Impacts of Climate Change on Runoffs in East Azerbaijan, Iran. Global and Planetary Change 78(3-4),137-146.

Zhan, X., Huang, M.L., 2004, ArcCN-Runoff: An ArcGIS tool for generating curve number and runoff maps, Environmental Modelling & Software 19, pp. 875–879.

Zhang, W., Sun, C., Qiu, Q., 2016. Characterizing of a capillary barrier evapotranspirative cover under high precipitation conditions. Environmental Earth Science 75(6). DOI 10.1007/s12665-015-5214-9.

Table 1. Input data used for model set-up and validation.

Data	Parameter	Period/ Resolution	Unit	Time scale	Data source	Application in
Meteorological	Precipitation	1961-2005	mm	daily	Iranian Meteorological Organization of East Azerbaijan Province (IMO)	SDSM and HELP
	Temperature	1961-2005	ºC			
	Solar radiation	1961-2005	MJ/M^2			HELP
	Average wind speed	1961-2005	km/h	annual		
	Relative humidity for every season	1961-2005	%	season		
Atmospheric	NCEP large scale data	1961-2005	mm & ºC	daily	https://esgf-node.llnl.gov/projects/cmip5/	SDSM
Raster	Digital Elevation Model	30m	m	2011	https://lpdaac.usgs.gov/products/astgtmv003	HELP
	Land use	10m		2016	Ghorbanian et al. (2020)	
	LAI	500m		4-day	MODIS: Product of MOD15A3H.006	
	Evapotranspiration	500m	mm	daily	MODIS: Product of MOD16A2.006	
Stratigraphic for soil data	Info. of piezometric logs profile	-	-	-	Forest, Rangeland and Watershed Management Organization of Azerbaijan Province	

Hydrological	Groundwater level	-	m	monthly	East Azerbaijan Regional Water Organization	

Table 2- Selection of large-scale predictor variables for predicting local precipitation and temperature parameters in Tabriz station.

Variable	**Selected Predictor**	**predictors Description**	**Absolute correlation**	**Partial correlation**
Temperature	Ncepmslpgl.dat	Mean sea level pressure	-0.74	-0.27
	Ncepp500gl.dat	500 hPa Geopotential	0.87	0.35
	Nceps850gl.dat	850 hPa Specific humidity	0.83	0.07
	Ncepshumgl.dat	Surface specific humidity	0.77	0.09
	Nceptempgl.dat	Air temperature at 2 m	0.97	0.46
Precipitation	Ncepp5_vgl.dat	500 hPa Meridional wind component	0.337	0.081
	Ncepp8zhgl.dat	850 hPa Divergence of true wind	-0.284	-0.026
	Ncepp8_vgl.dat	850 hPa Meridional wind component	0.256	0.041
	Ncepp850gl.dat	850 hPa Geopotential	-0.264	-0.043
	Nceps500gl.dat	500 hPa Specific humidity	0.22	0.03

Table 3. Evapotranspiration and recharge changes under assumed LAI for the baseline period (1961-2005).

Leaf area index	**0.1**	**0.5**	**1**	**1.5**	**2**	**2.5**	**3**	**3.5**	**4**	**4.5**	**5**
Evapotranspiration (%)	82	84	86	86	88	89	90	92	93	93	94
Groundwater recharge (%)	12	10	9	9	8	7	7.6	7	7	6	6

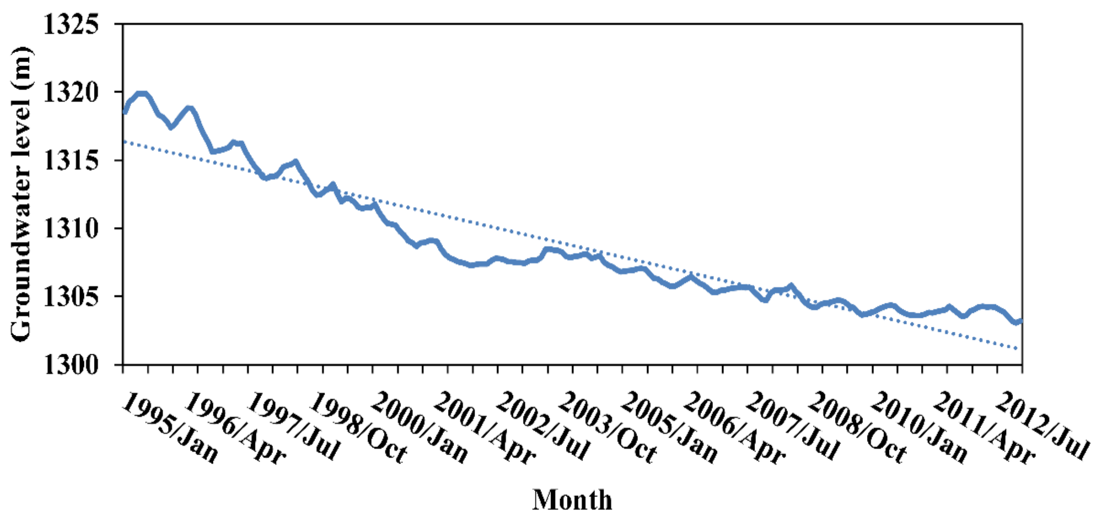

Fig. 1. Groundwater level (in meters above mean sea level) over the period 1995-2012 in Tasuj plain aquifer, Iran.

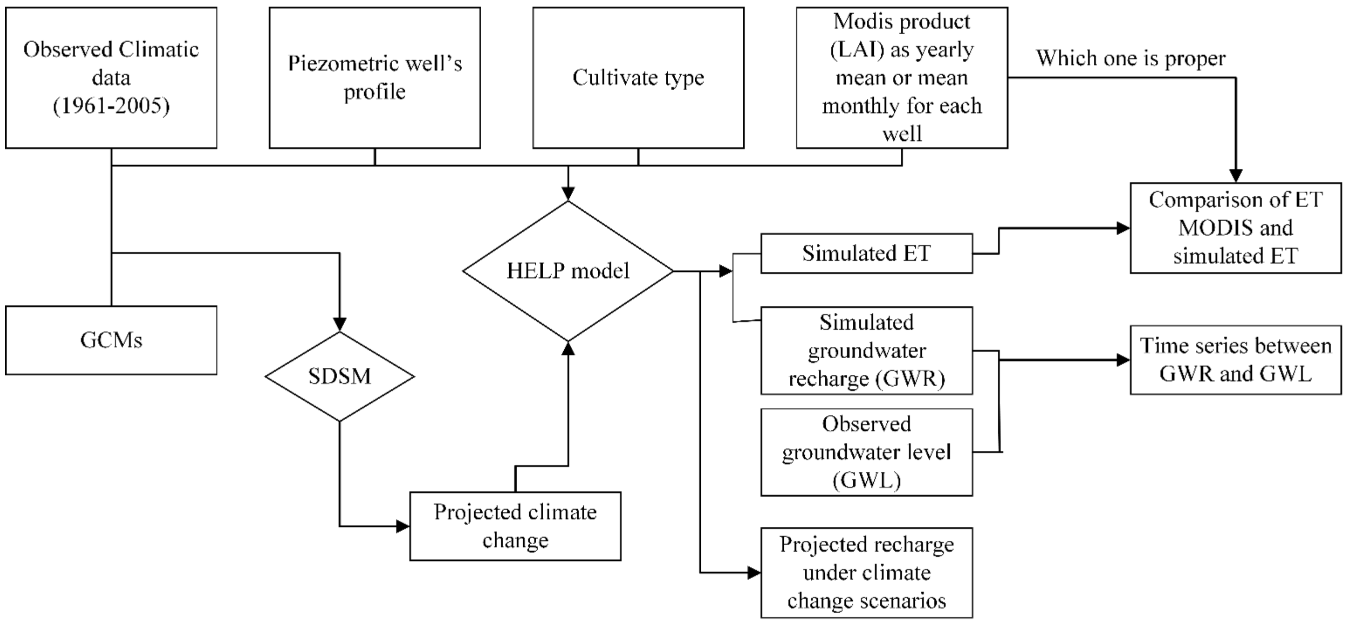

Fig. 2. An overview of the proposed method.

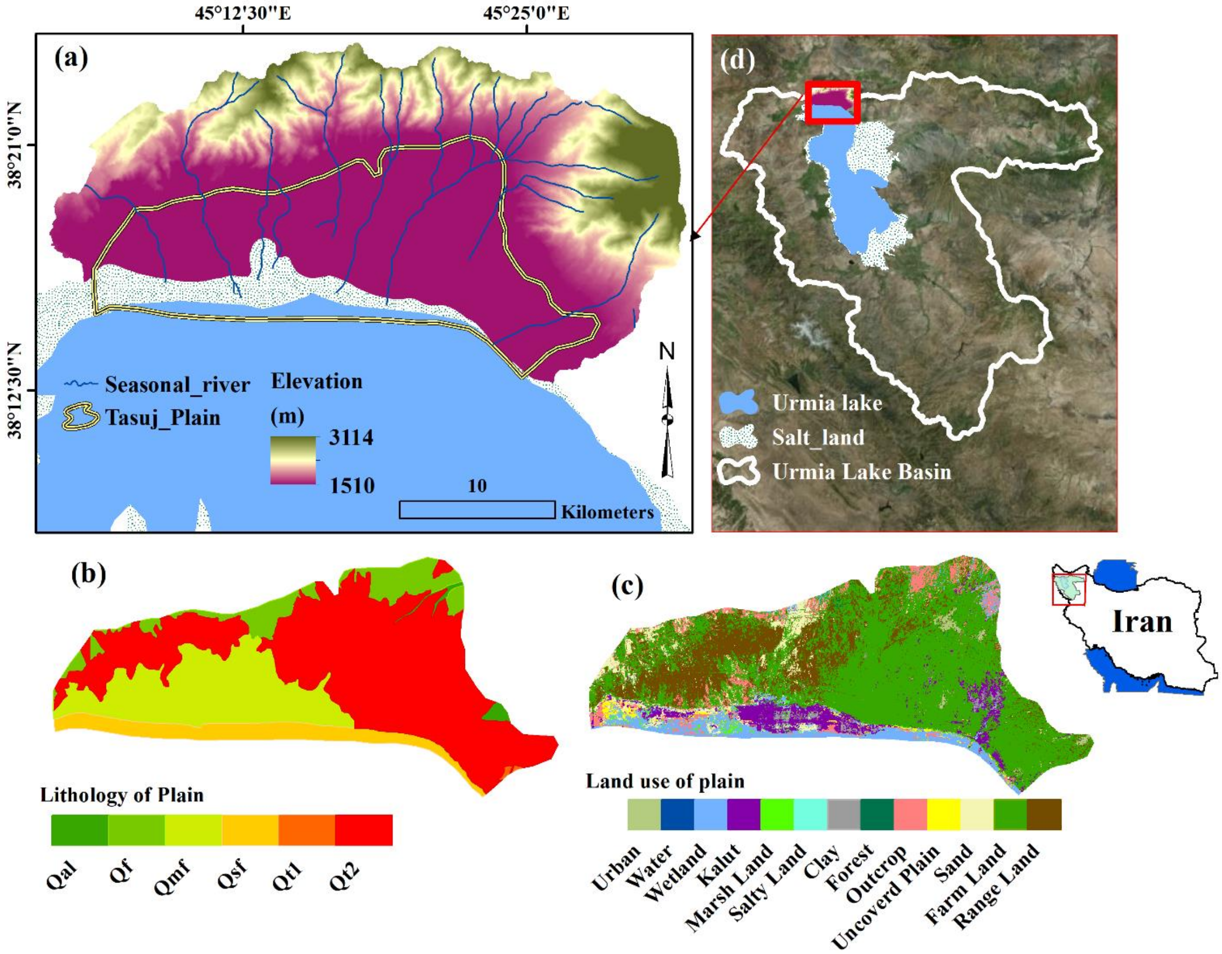

Fig. 3. (a): Tasuj catchment, elevation and stream system, (b) lithology including Qal = recent alluvium (1%), Qf = Gravel fan (10%), Qmf = sandy salty flats (24%), Qsf = salt flats (9%), Qt1 = high level terraces (0.5%), Qt2 = old terraces (55.5% of the plain area)), (c): land use for the year 2017 (Gorbanian et al., 2020) (d): Urmia Lake basin.

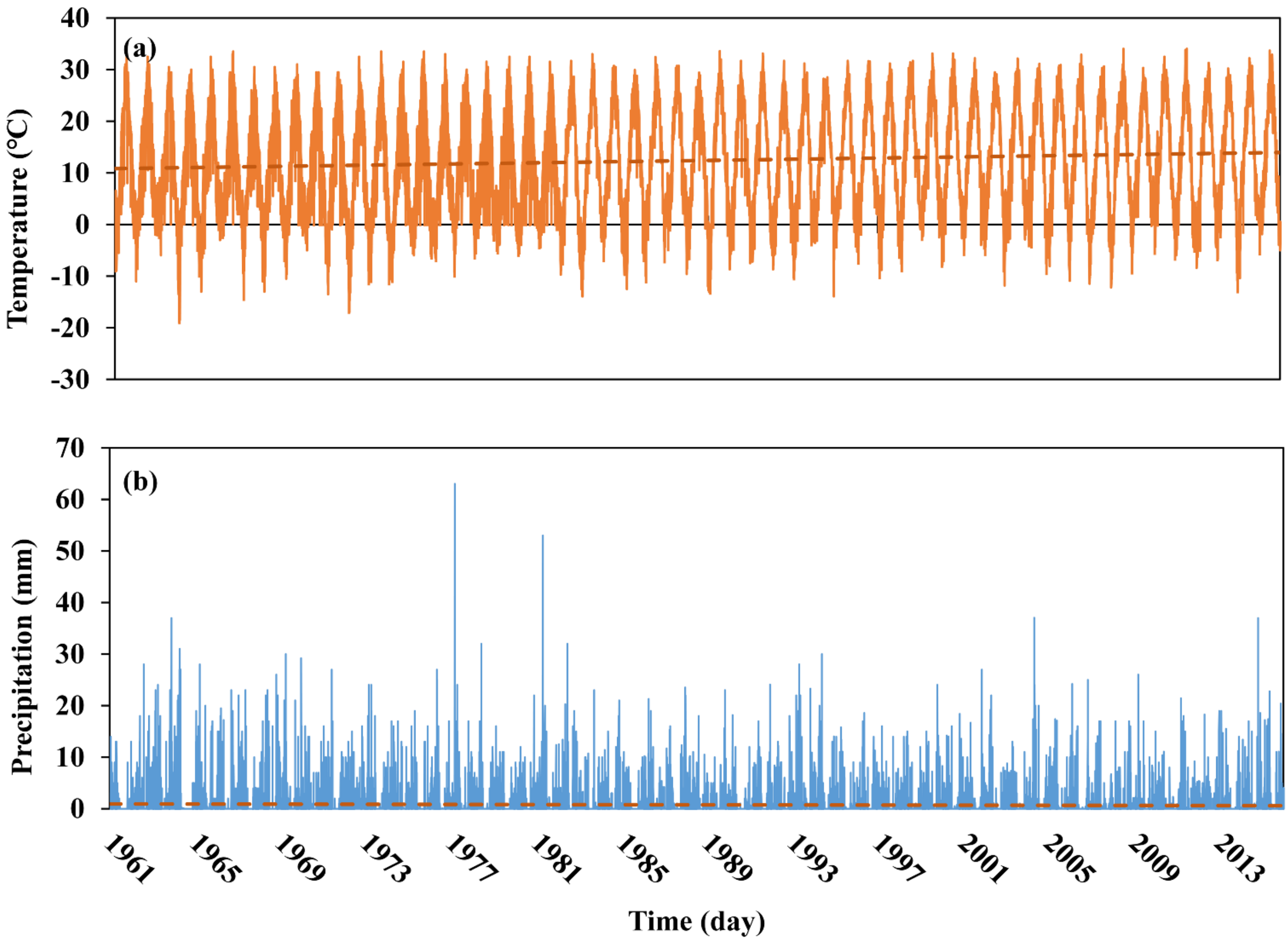

Fig. 4. Daily time series of mean temperature and precipitation from 1961-2015 in Tabriz station. The linear trend is shown by the dashed lines.

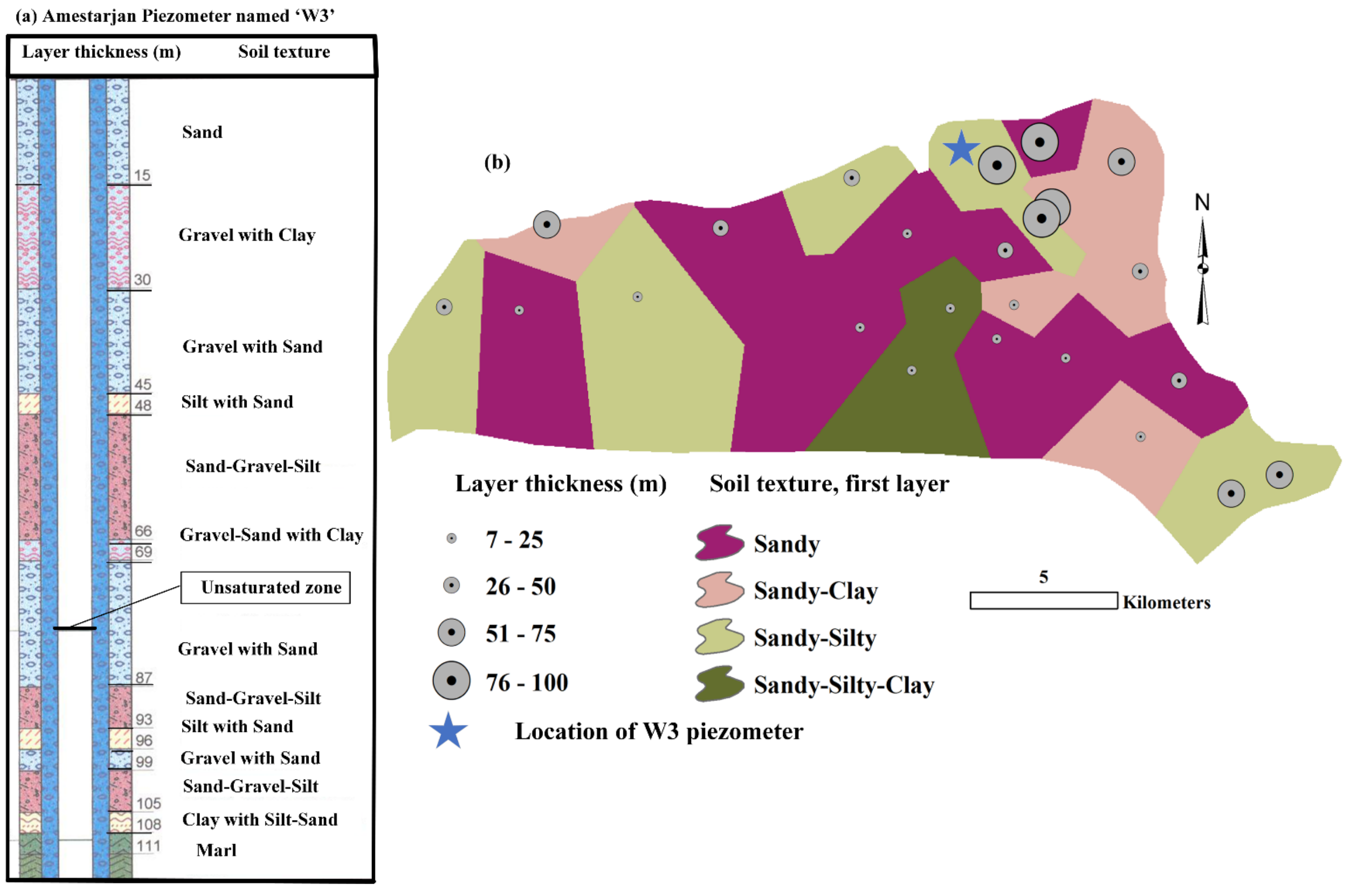

Fig. 5. (a) Shows the soil texture map in the first layer and soil layer thickness through piezometric logs and (b) a sample schematic (stratigraphic) of a log.

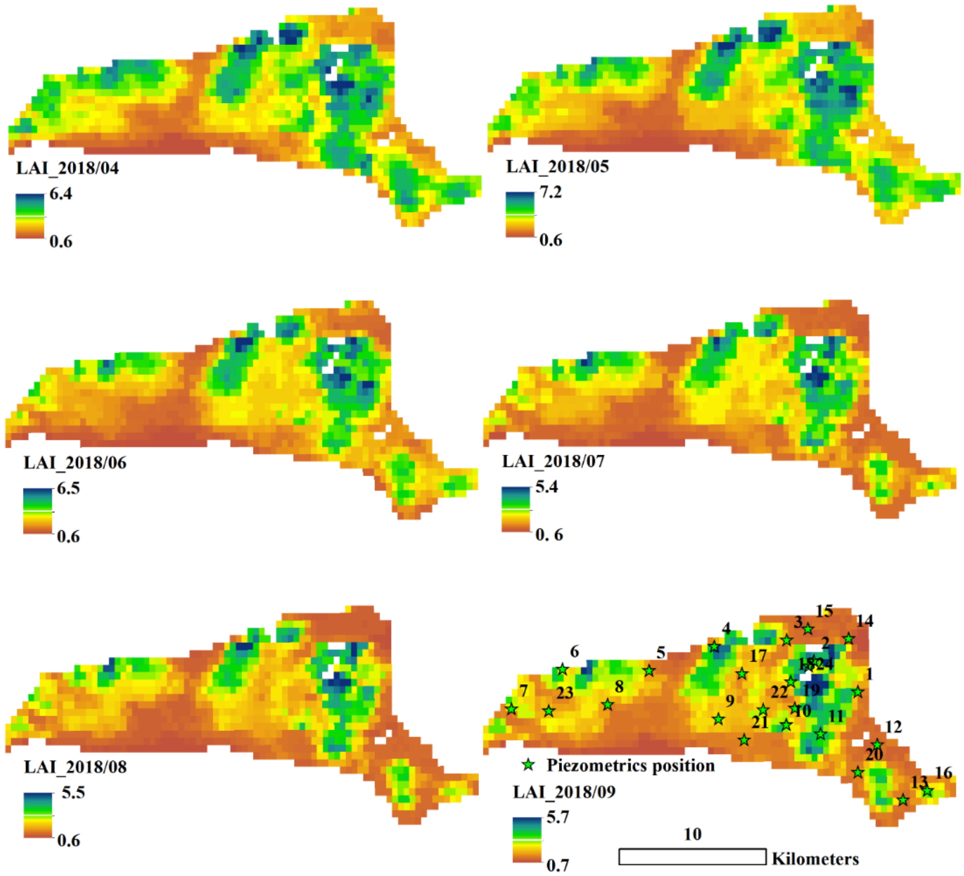

Fig. 6. Leaf area index (LAI) in 2003 was obtained from MODIS product for each well of W1-W24.

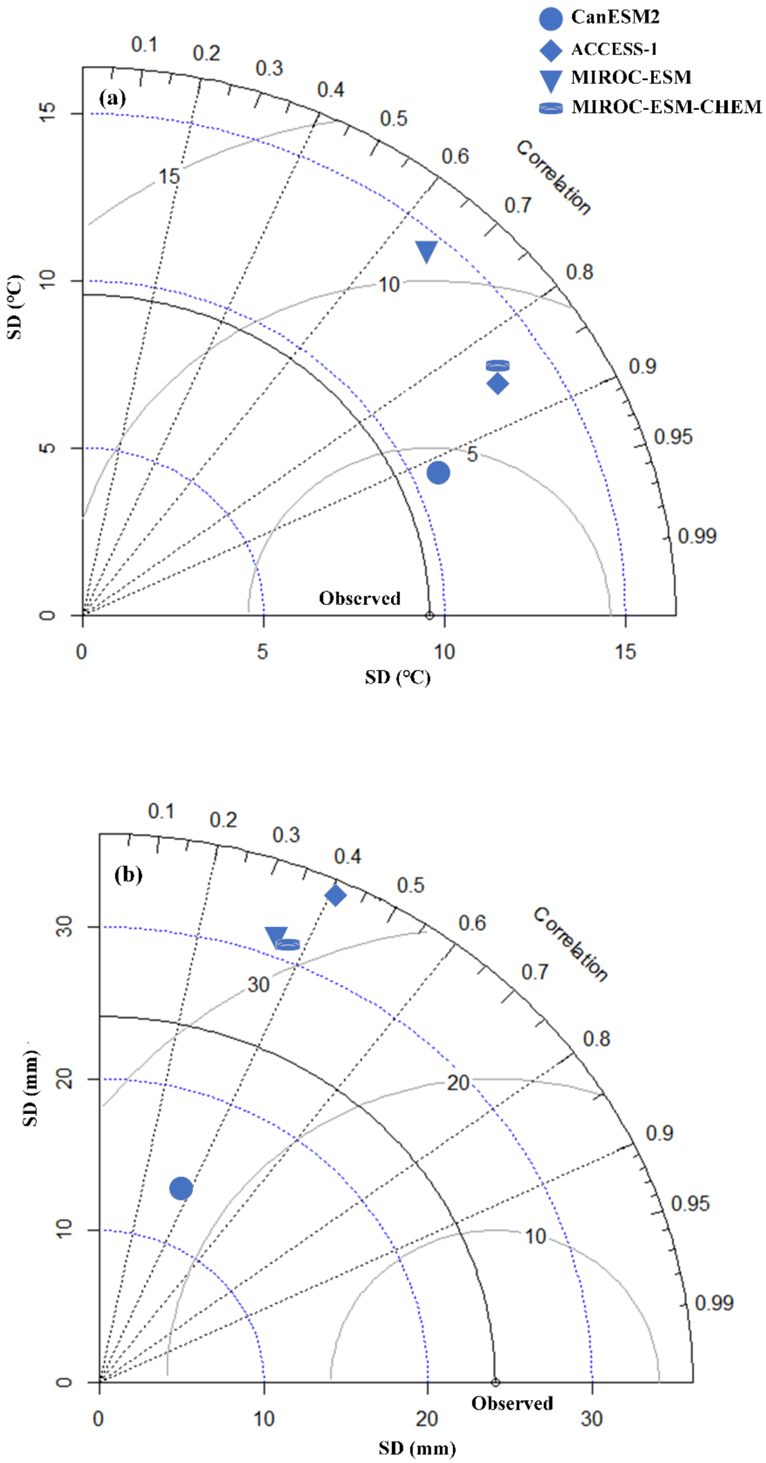

Fig. 7. Taylor diagrams of the monthly climate variables, (a) temperature (b) precipitation.

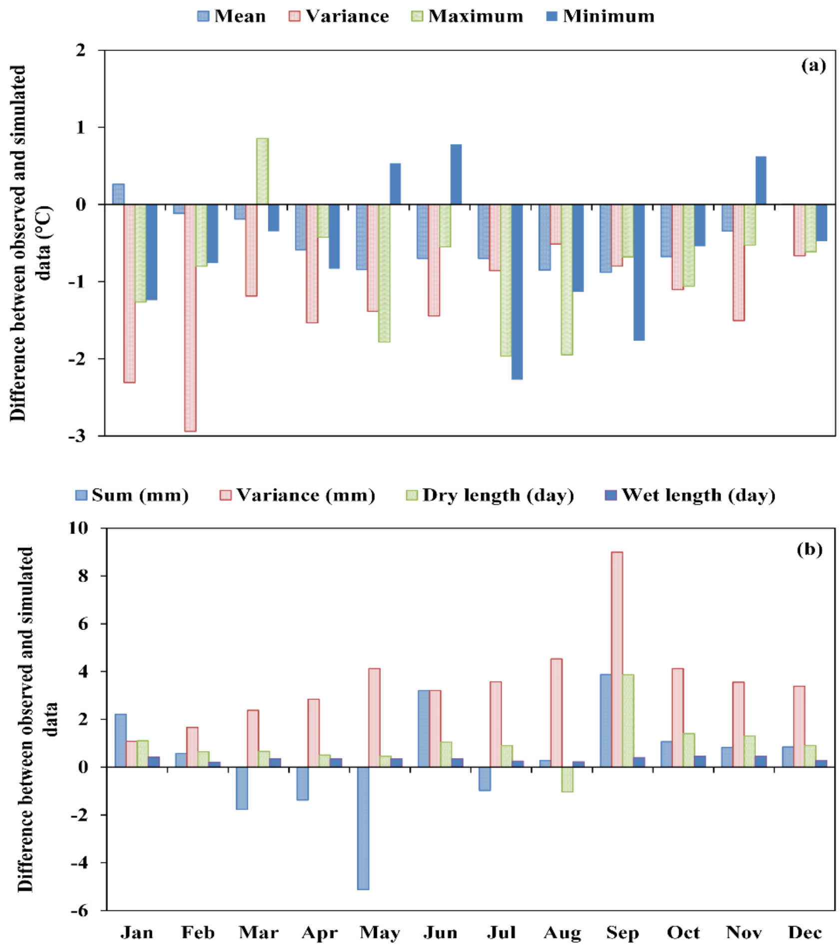

Fig. 8. Difference between observed and simulated: (a) temperature, and (b) precipitation (1961-2005).

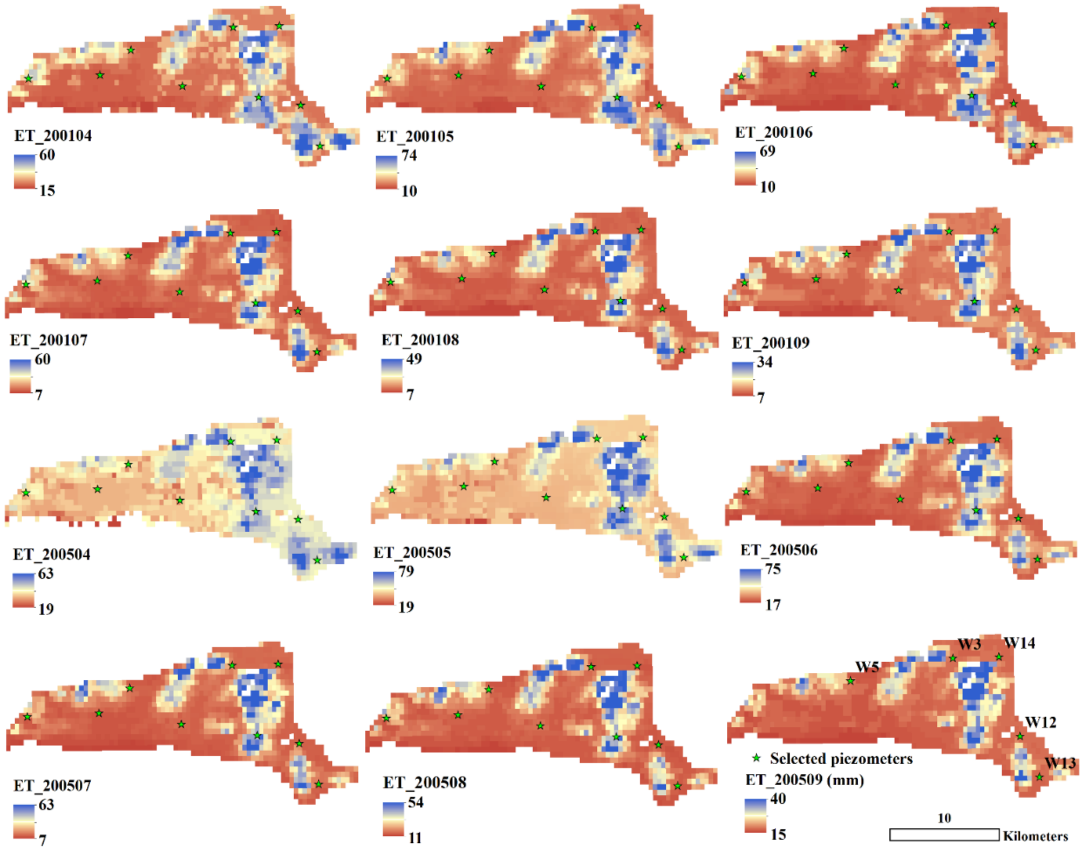

Fig. 9. Spatiotemporal variations of ET in the Tasuj plain catchment from April (200104 in the legend means the April of 2001) to September (200109 means the September of 2001) during the period 2001 and 2005 based on MODIS ET and selected piezometer wells for the verification of estimated ET from the HELP model.

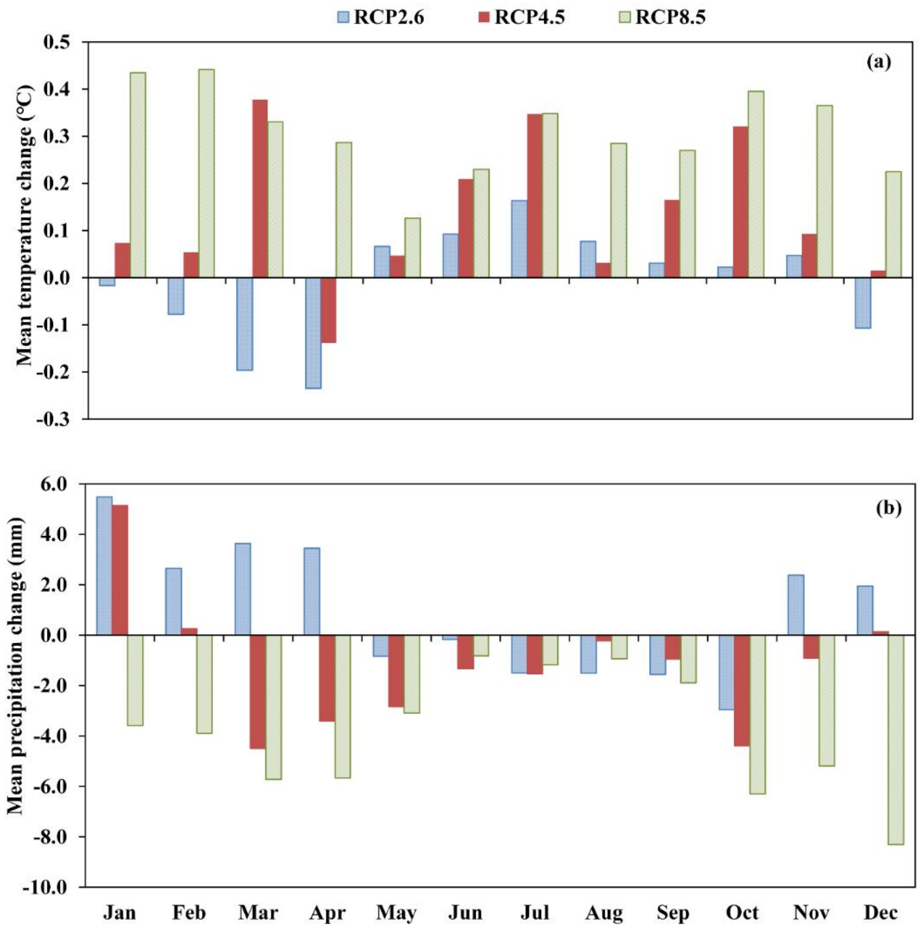

Fig. 10. Near future changes (2017-2030): (a) in temperature, and (b) precipitation; under RCP2.6, RCP4.5, and RCP8.5 scenarios for Tabriz station compared to the base period (2005-1961).

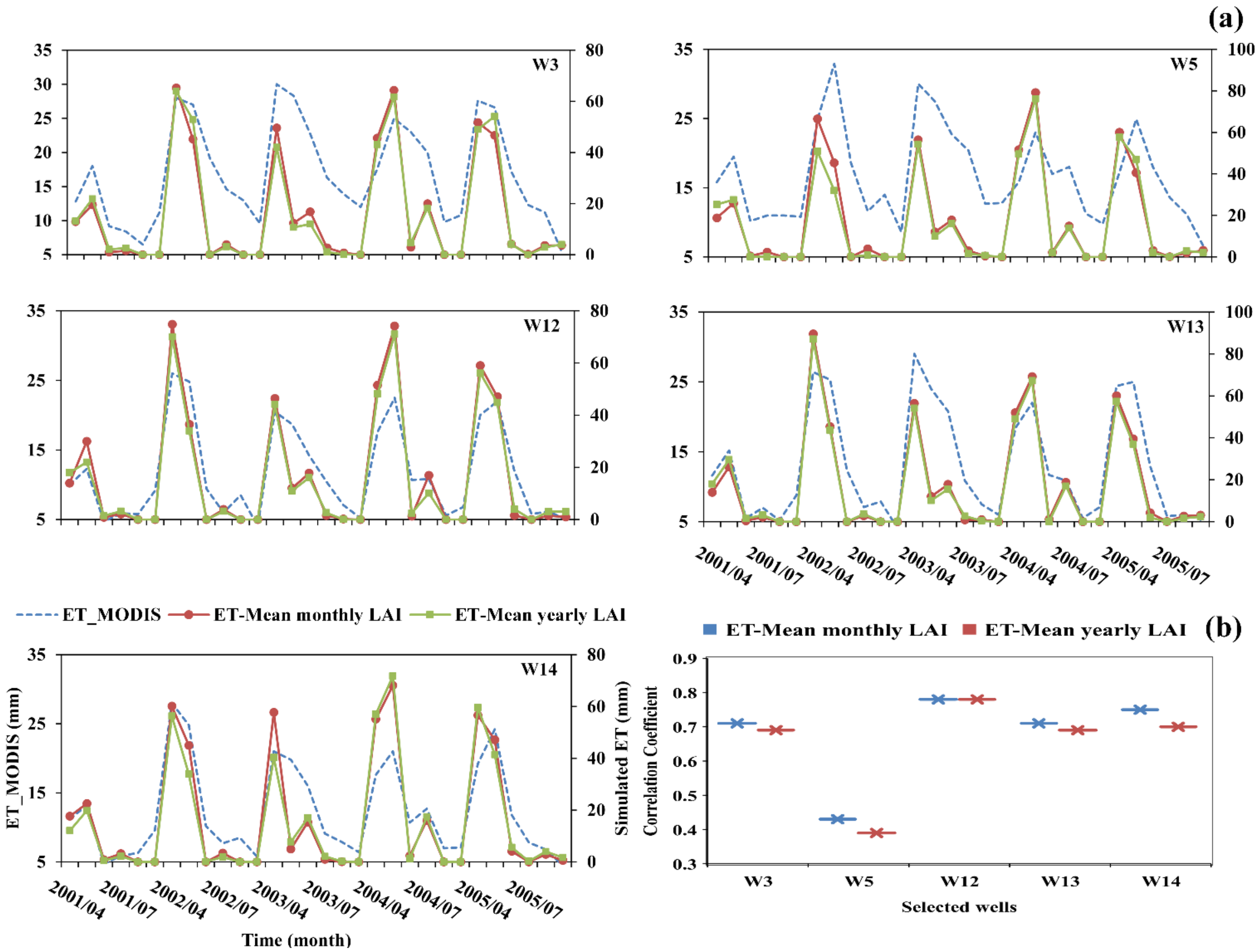

Fig. 11. (a) Comparison of MODIS ET and simulated ET using HELP over 2001-2005 at a monthly scale (the growing season) under mean yearly and mean monthly LAI values. (b) Shows the correlation coefficient between MODIS ET and simulated ET using mean yearly and mean monthly LAI values in the selected wells for testing.

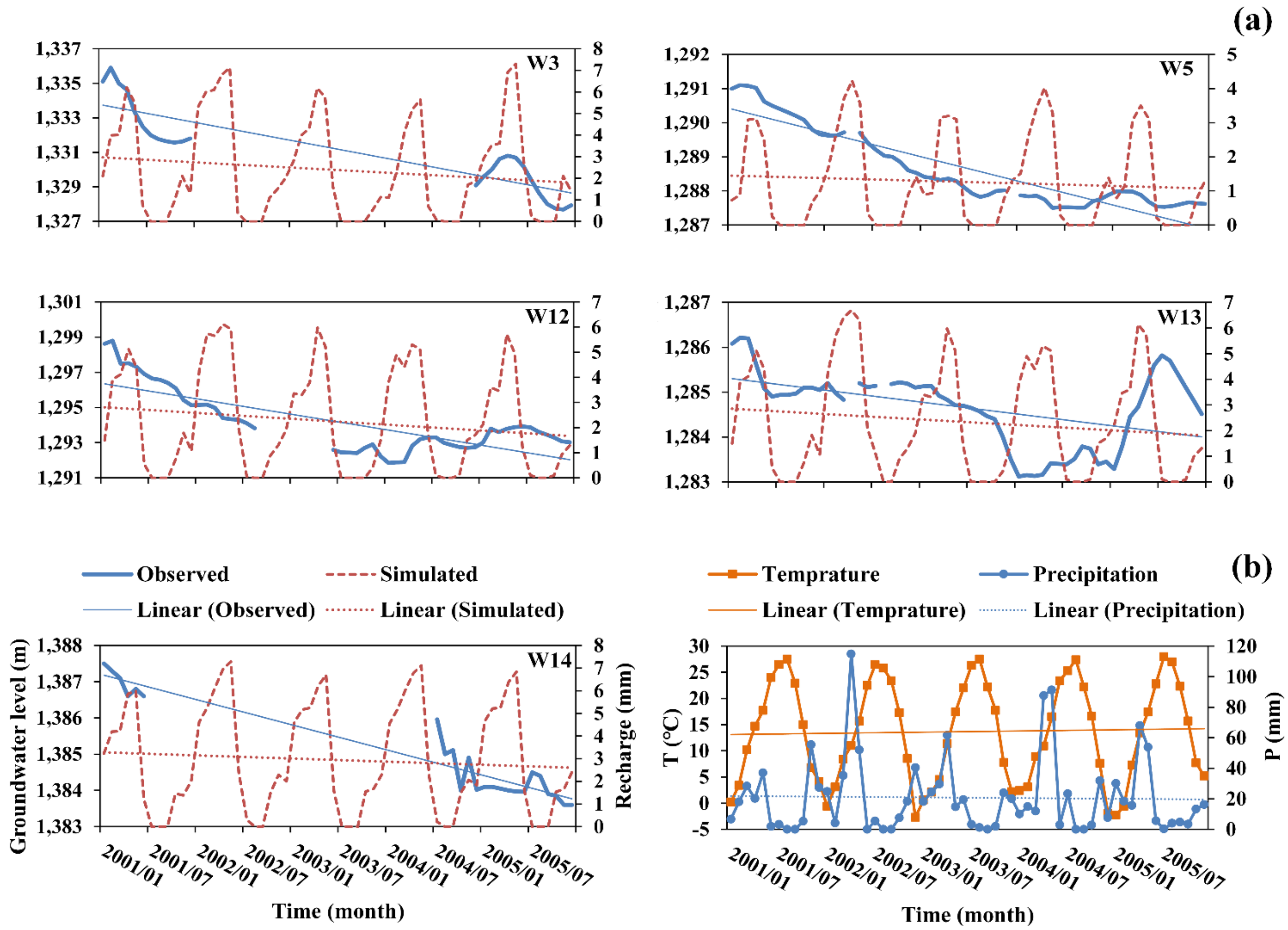

Fig. 12. Compression observed groundwater level and simulated recharge in selected piezometric wells and temperature and precipitation variations over 2001-2005.

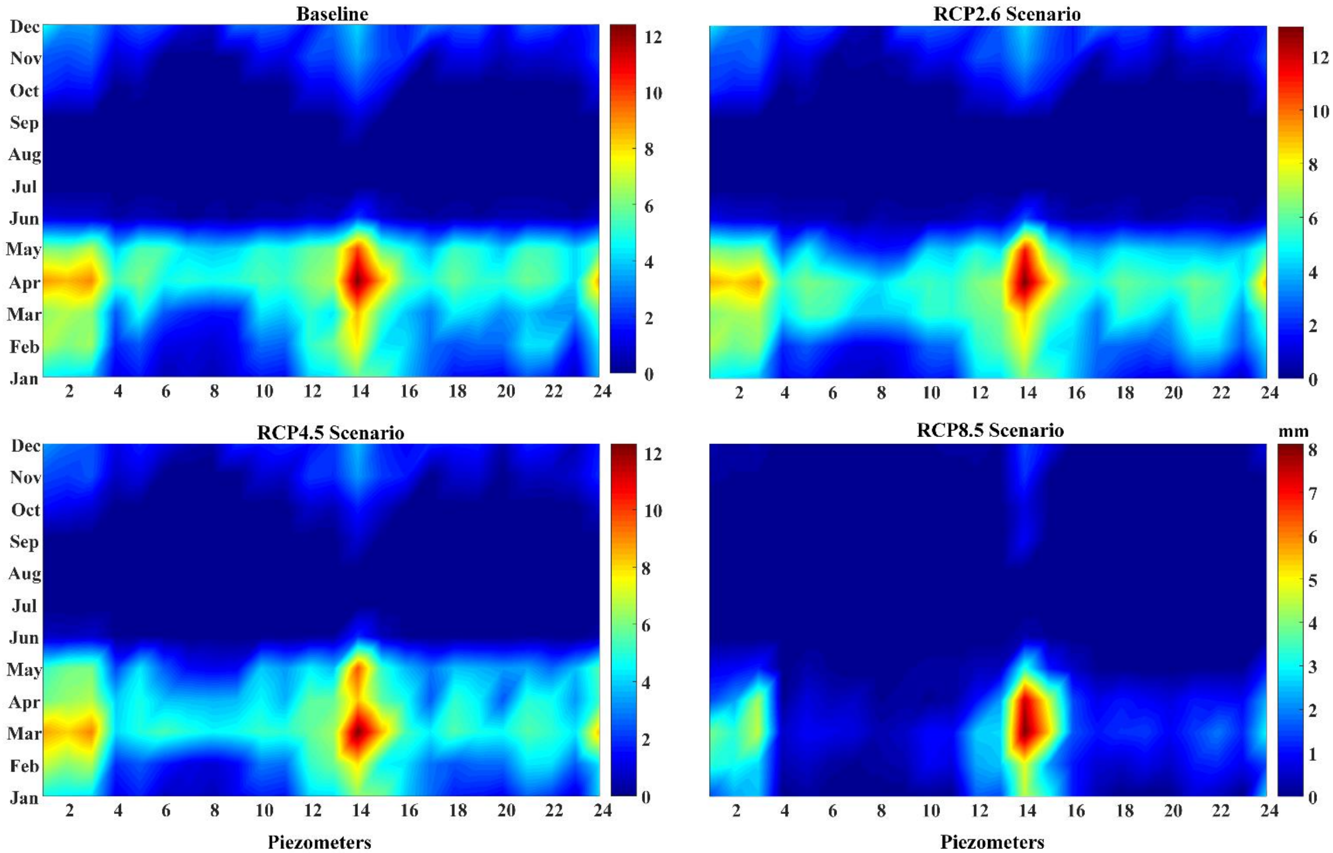

Fig. 13. Mean monthly recharge (estimated using HELP) in the baseline (1961-2005) and under climate change scenarios over 2017-2030 at the piezometers of the Tasuj plain.

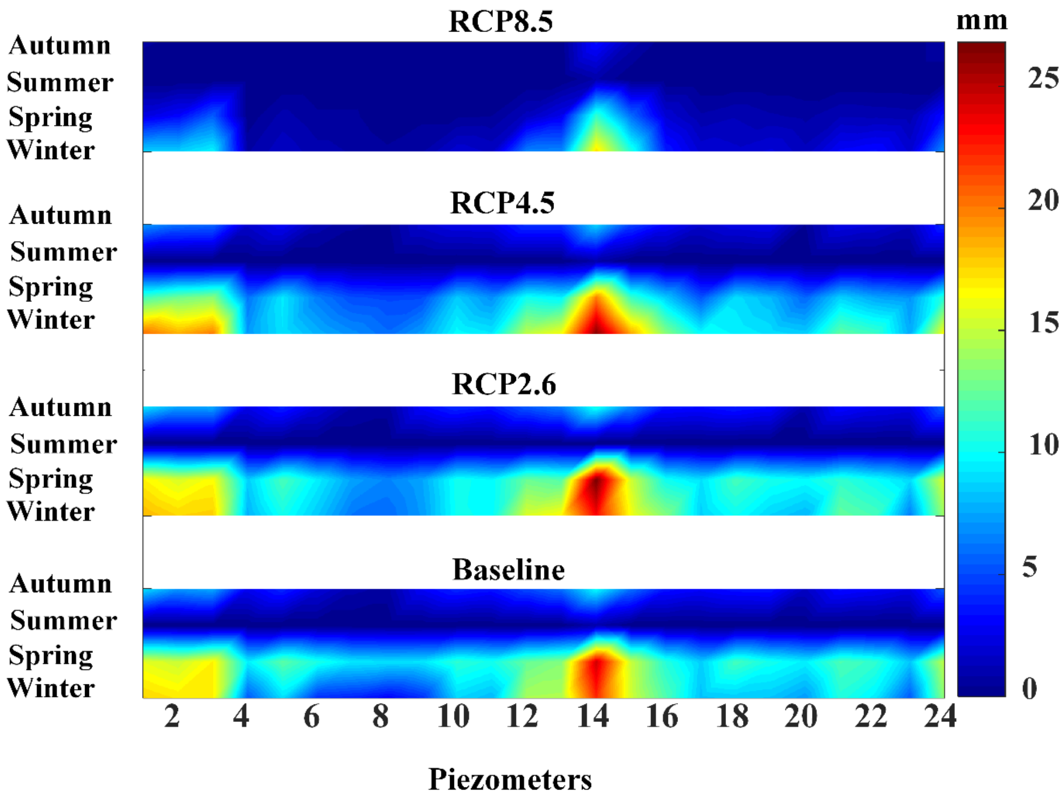

Fig. 14. Seasonally variation in 2030 at piezometers of W1- W24.

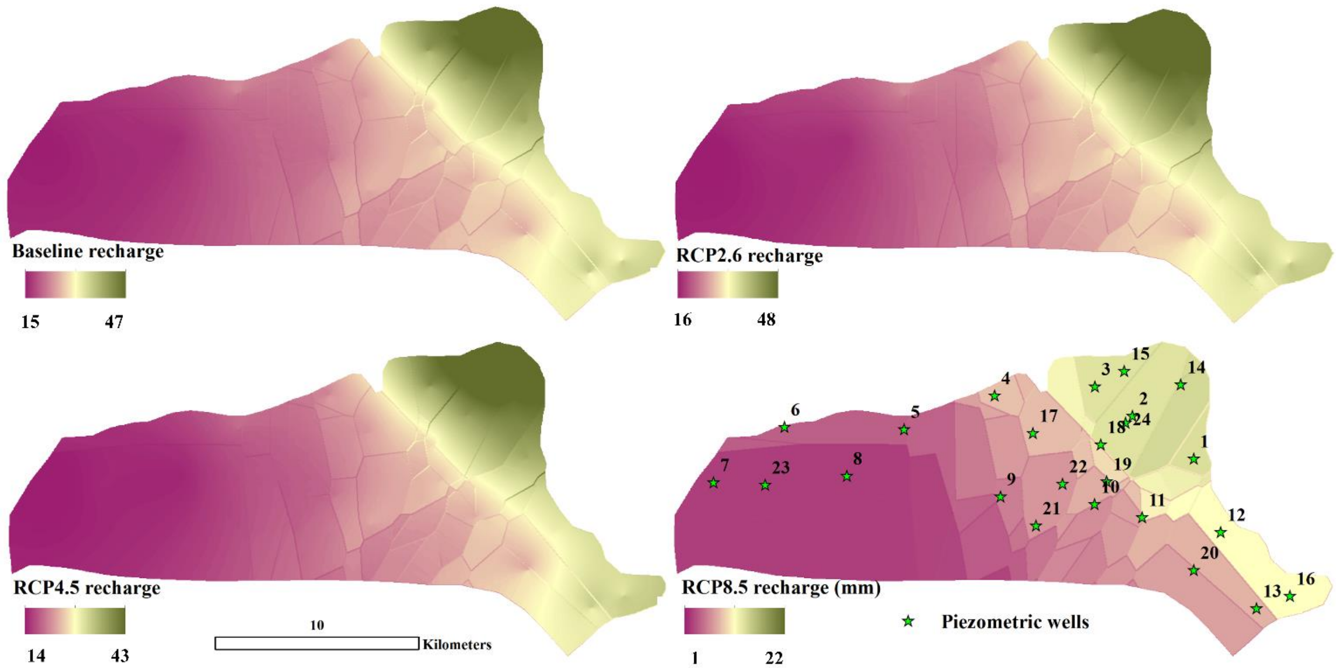

Fig. 15. Annual variation of groundwater recharge based on climate change scenarios at W1-W24 in the Tasuj plain, Iran in 2030.